Sequence Dependence of Excess Electron Transfer in DNA†

Kazuki Tainaka,‡ Mamoru Fujitsuka, Tadao Takada, Kiyohiko Kawai, and Tetsuro Majima*

The Institute of Scientific and Industrial Research (SANKEN), Osaka University, Mihogaoka 8-1, Ibaraki, Osaka 567-0047, Japan

Received: March 18, 2010; Revised Manuscript Received: May 14, 2010

DNA-mediated charge transfer has recently received a substantial attention because of its biological relevance in the DNA damage and DNA repair as well as the potential applications to nanoscale electronic devices. In contrast to the numerous mechanistic studies on oxidative hole transfer (HT) through DNA, our understanding of reductive electron transfer process still remains limited. In this article, we demonstrate the results of direct observation of the excess electron transfer (EET) through DNA, which conjugated with aminopyrene (**^{A}Py**) and diphenylacetylene (**DPA**) as a photosensitizing donor and an acceptor of excess electron, respectively. By inserting dihydrothymine as a spacer between **^{A}Py** and T or C, the yield of electron arrival to **DPA** was improved. It was indicated that EET through DNA completed within a few or a few tens nanosecond time scale even for EET over 34 Å for both consecutive T and C sequences. The various factors such as mismatch sequence and DNA length on the yield of electron arrival to **DPA** were examined.

Introduction

The DNA scaffold, which is one of the programmed self-assemblies consisting of π-conjugated systems, is expected to provide an attractive tool to construct nanoscale wires of electronic component.[1] Although the understanding of DNA-mediated electron transfer has been focused on the oxidative electron transfer,[2−5] the hole transport (HT) in DNA has profound drawbacks with the respect to electronic devices; simultaneous DNA damage and slow rate of hole migration in a sequence including G. On the contrary, the excess electron transport (EET) in DNA is more promising for the application in electronic devices because of the lack of DNA lesion and the involvement of all base pairs (C•G and T•A) as intermediate electron carriers.[6,7] Therefore, mechanistic studies of EET in DNA would be quite worthwhile for the development of molecular electronic devices.

Recent studies have provided global mechanistic insights into EET process based on the photochemical product analysis. Initially, Carell and co-workers established the evaluation system for EET in DNA utilizing flavin and T•T dimer as a photoexcitable electron donor and chemical electron trap, respectively,[8−10] and proposed a thermally activated electron hopping mechanism.[11−14] Rokita and Ito suggested a similar mechanism in the other donor−acceptor system containing aromatic amine and 5-bromo-2′-deoxyuridine, which is most widely applied as a kinetic electron trap.[15,16] Stafforst and Diderichsen have investigated EET in DNA-PNA by chemical monitoring using thymine oxetane.[17] More recently, Barton and co-workers compared the efficiency of the hole and electron migration process within the same assembly containing Ir(III) complex[18,19] which enables the initiation of hole and electron injection into DNA bases, and demonstrated that the both processes showed remarkably shallow distance dependence.[20] Kobayashi and his co-workers reported the contribution of $(A•T)^{•-}$ in the stabilization of excess electron induced by pulse radiolysis.[21]

Time-resolved absorption measurements during laser flash photolysis have mainly offered fundamental kinetics of electron injection process. Lewis, Wasielewski, and co-workers investigated the kinetics of the photoinduced electron injection into DNA hairpins capped with a stilbene diether derivative.[22] Pyrene-modified pyrimidines were also synthesized to monitor the initial charge transfer process between pyrene and pyrimidines by Netzel group[23,24] and Wagenknecht group.[25,26] As an alternative system, Fiebig and co-workers developed DNA conjugates with the ethidium derivative as a base pair surrogate, and suggested that the rates and distance dependencies of EET and HT in DNA were closely associated with nuclear motions and conformational flexibility.[27] Lewis, Fiebig, and their co-workers recently reported the laser flash photolysis study on electron injection from aminopyrene to DNA, while electron transfer among the DNA was analyzed by means of product analysis.[28,29]

In the previous paper,[30] we have investigated the EET in naphthalimide (NI) conjugated DNA by using pulse radiolysis experiments, in which injected excess electron on DNA was expected to move to NI to form NI radical anion. Unfortunately, the rate constant of EET was not obtained, because the kinetic trace of the transient absorption of NI radical anion showed generation behavior with the same rate as the collision of solvated electron with DNA, indicating a rapid EET. From the amount of generated radical anion, we suggested that the number of electron hopping or extent of electron tunneling is limited. For clarification of details of excess electron transfer such as extent of electron hopping and sequence dependece, further investigation using laser flash photolysis is indispensable. On the other hand, we accomplished an efficient generation of a long-lived hole escaped from charge recombination into DNA by using the consecutive adenine sequence which facilitates the rapid and directional hole transport, and succeeded in the direct observation of HT in DNA over 100 Å.[31] Analogously, it is expected that by conjugation of additional chromophore, which traps injected excess electron, to DNA as shown in Figure 1,

† Part of the "Michael R. Wasielewski Festschrift".

* To whom correspondence should be addressed. E-mail: majima@sanken.osaka-u.ac.jp.

‡ Present address: Institute of Advanced Energy, Kyoto University, Gokasho, Uji, Kyoto 611-011, Japan.

10.1021/jp1024685
Published on Web 05/28/2010

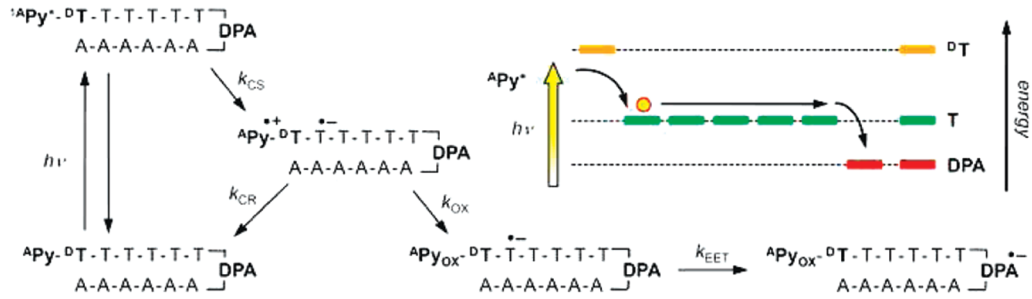

Figure 1. Conceptual illustration of the strategy for the imperative generation of an "orphan" excess electron escaped from charge recombination, and the directional electron migration through DNA modified with alkylamino-modified pyrene (**APy**), dihydrothymidine (**DT**), and diphenylacetylene (**DPA**). These processes are photoinduced charge separation (k_{CS}), charge recombination (k_{CR}), irreversible inactivation of **APy** radical cation via iminium cation (k_{OX}), and excess electron transfer (k_{EET}) in DNA.

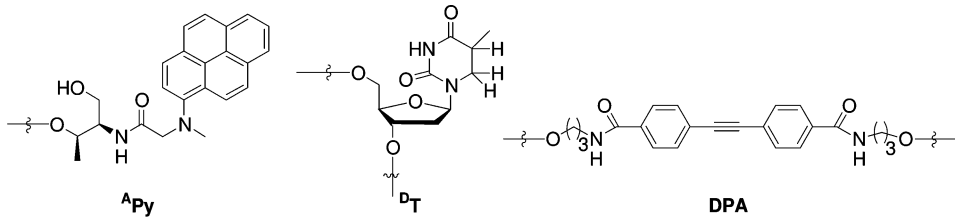

dyad conjugate

APy-N; N = A, C, G, or T

hairpin no.	sequence	hairpin no.	sequence
1	**APy**-TTTT-**DPA**-AAAA	15	**APy**-**D**T-TCTCT-**DPA**-AGAGAA
2	**APy**-**D**T**D**T-TT-**DPA**-AAAA	16	**APy**-**D**T-CCCCC-**DPA**-GGGGGA
3	**APy**-**D**T-TTT-GAA-AAAA	17	**APy**-**D**T-TTGTT-**DPA**-AACAAA
4	**APy**-**D**T-TTT-**DPA**-AAAA	18	**APy**-**D**T-TGTGT-**DPA**-ACACAA
5	**APy**-TTTTT-GAA-AAAAA	19	**APy**-**D**T-TTTT-**DPA**-AAAAA
6	**APy**-TTTTT-**DPA**-AAAAA	20	**APy**-**D**T-TTTTTT-**DPA**-AAAAAAA
7	**APy**-**D**T-TTTTT-GAA-AAAAAA	21	**APy**-**D**T-TTTTTTT-**DPA**-AAAAAAAA
8	**APy**-**D**T-TTTTT-**DPA**-AAAAAA	22	**APy**-**D**T-TTTTTTTT-**DPA**-AAAAAAAAA
9	**APy**-T-**D**T-TTTT-**DPA**-AAAAAA	23	**APy**-**D**T-CCC-**DPA**-GGGA
10	C-**D**T-TTTTT-**DPA**-AAAAAAG	24	**APy**-**D**T-CCCC-**DPA**-GGGGA
11	**APy**-**D**T-TTTTT-**DPA**-AATAAA	25	**APy**-**D**T-CCCCCC-**DPA**-GGGGGGA
12	**APy**-**D**T-TTTTT-**DPA**-AACAAA	26	**APy**-**D**T-CCCCCCC-**DPA**-GGGGGGGA
13	**APy**-**D**T-TTTTT-**DPA**-AAGAAA	27	**APy**-**D**T-CCCCCCCC-**DPA**-GGGGGGGGA
14	**APy**-**D**T-TTCTT-**DPA**-AAGAAA		

Figure 2. (Upper) Structures of **APy** as an electron donating photosensitizer, **DT** as a spacer, and **DPA** as an electron acceptor. (Lower) Dyad conjugates and a series of synthetic DNA hairpins modified with **APy**, **DT**, and **DPA**.

various information on EET such as kinetics and extent of electron transfer will be clarified. In this paper, we demonstrate the results of direct observation of EET through DNA with donor−acceptor system consisting of diphenylacetylene (**DPA**) bridged hairpins tethering dimethylaminopyrene (**APy**) at the 5′-end (Figure 2).

Experimental Section

DNA Synthesis. Cyanoethyl phosphoramidite of dihydrothymine (**DT**) and **DPA** were synthesized as previously reported.[32,33] According to Scheme S1 of Supporting Information, cyanoethyl phosphoramidite of **APy** was synthesized. All the other reagents for DNA synthesis were purchased from Glen Research. Hairpin DNAs used in this study were synthesized on an Applied Biosystems 3400 DNA synthesizer with standard solid-phase techniques and purified on a JASCO HPLC with a reversed-phase C-18 column with an acetonitrile/50 mM ammonium formate gradient. The DNAs were characterized by digestion with nuclease P1 and alkaline phosphatase (AP) and by MALDI-TOF mass spectra.

Laser Flash Photolysis Experiments. The subpicosecond transient absorption spectra were measured by the pump and probe method using a regeneratively amplified titanium sapphire laser (Spectra Physics, Spitfire Pro F, 1 kHz) pumped by a Nd:YLF laser (Spectra Physics, Empower 15) for an aqueous solution containing 450 μM hairpin DNA, 100 mM NaCl, and 10 mM Na phosphate buffer (pH 7.0). The seed pulse was generated by the titanium sapphire laser (Spectra Physics, Tsunami 3941-M1BB, full width at half-maximum (fwhm) 80 fs, 800 nm). Excitation pulse at 360 nm was generated by optical parametric amplifier (Spectra Physics, OPA-800CF). A white continuum pulse, which was generated by focusing the residual of the fundamental light to a flowing water cell after a computer-controlled optical delay, was divided into two parts and used

as the probe and the reference lights, of which the latter was used to compensate the laser fluctuation. The both probe and reference lights were directed to a rotating sample cell with 1.0 mm of optical path and were detected with a charge-coupled device detector equipped with a polychromator (Solar, MS3504). The pump pulse was chopped by a mechanical chopper synchronized to one-half of the laser repetition rate, resulting in a pair of the spectra with and without the pump, from which absorption change induced by the pump pulse was estimated. The nanosecond transient absorption measurements were performed using the LFP technique[31,34] for an aqueous solution containing 110 μM hairpin DNA, 100 mM NaCl, and 10 mM Na phosphate buffer (pH 7.0). The third-harmonic oscillation (355 nm, fwhm of 4 ns, 10 mJ/pulse) from a Q-switched Nd:YAG laser (Continuum, Surelite II-10) was used for the excitation light. A xenon flash lamp (Osram, XBO-450) was focused into the sample solution as the probe light for the transient absorption measurement. Time profiles of the transient absorption in the UV−vis region were measured with a monochromator (Nikon, G250) equipped with a photomultiplier (Hamamatsu Photonics, R928) and digital oscilloscope (Tektronics, TDS-580D). Obtained kinetic signals were simply analyzed by single-exponential fits to determine the apparent excess electron transfer mechanism.

TABLE 1: Fluorescence Quantum Yields (Φ_{fl}), Quenching Efficiency (Q_{eff}), and Subpicosecond Transient Data from Water-Soluble ^{A}Py Monomer and ^{A}Py·N (N = A, C, G, or T) Dyad Conjugates[a]

sample	Φ_{fl}[b]	Q_{eff}	507 nm τ, ps[c]	560 nm τ, ps[d]	507/560, ps[e]
^{A}Py monomer[f,g]	0.252				
^{A}Py·A	0.110	0.56	325	376	n.d.
^{A}Py·C	0.031	0.88	1.07[g] 9.23	5.69	4.05
^{A}Py·G[g]	0.244	0.03	409	408	n.d.
^{A}Py·T	0.016	0.94	0.60[h] 6.48	2.49	2.14

[a] Measurements were performed in 20 mM sodium phosphate, 100 mM sodium chloride (pH 7.0) buffer solution. [b] Quantum yields were determined from emission spectra excited at 360 nm by using coumarin dye as a reference. [c] Decay times for the transient absorption of ^{A}Py$^{\bullet+}$ corresponded to charge recombination. [d] Decay times for the transient absorption of ^{A}Py*. [e] Rise time for the 507/560 band intensity ratio corresponded to electron injection from ^{A}Py* to a nucleobase. [f] Water-soluble ^{A}Py monomer (compound 7 in materials section of Supporting Information). [g] Measurements were performed in 20 mM sodium phosphate, 100 mM sodium chloride (pH 7.0) buffer solution containing 10% methanol. [h] Rise component attributed to the formation of ^{A}Py$^{\bullet+}$ in the presence of ^{A}Py* decay component.

Results and Discussion

Design of the DNA Sequence and Electron-Donating Photosensitizer for Observation of the Electron Arrival Process. For the direct observation of the electron arrival process through DNA, it is necessary to suppress the inactivation of the injected excess electrons by charge recombination after initial charge separation. To retard charge recombination of electron-donating a photosensitizer and injected excess electron, we examined following two issues. One is putting a redox-inactive intervening base pair as a spacer between a photosensitizer and a nucleotide initially oxidized. Another is utilization of irreversible electron injector.

The first issue is established in the case of HT in DNA. The oxidation of adenine (A) by the guanine (G) radical cation is endothermic because of the significant difference in the oxidation potential between G and A, and the hole hopping over consecutive A bases occurred very rapidly (>10^8 s^{-1}). Therefore, by placing the adequate nucleotide, which acts as a spacer, in the vicinity of the photosensitizer, the sufficient retardation of the initial charge-recombination process facilitates the directional HT through DNA.[35,36] However, in the case of EET, since pyrimidine bases as an excess electron carrier exhibit the comparable reduction potentials,[37] alternative contrivance is required. Dihydrothymine (^{D}T),[32] which is a major radiolysis product of thymine, appears to retain proper base pairing ability with adenine[38] and can be used as a spacer between donor and DNA.[39] Therefore, it is anticipated that insertion of ^{D}T·A base pair between the photosensitizing donor and the adjacent pyrimidine would cause the delay of the initial charge recombination rate, and result in the enhancement of the yield for electron arrival to DPA (Figure 1).

Another approach for enchancement of the yield for electron arrival to DPA will be utilization of irreversible electron injection as employed in the studies based on product analysis.[8−12,17−19] Here, we examined an electron-donating photosenstizer, whose radical cation was rapidly deactivated by the subsequent chemical reaction over the charge-recombination process. Alkylamino-modified donor could be hydrolyzed rapidly ($\sim 10^8$ s^{-1}) via iminium cation as an intermediate after the formation of radical cation in the competition with the back electron transfer.[40,41] As described above, pyrene derivatives have been used as photoexcitable electron donors because pyrene chromophore is able to reduce pyrimidine bases. Accordingly, we devised a dimethylamino-modified pyrene as an electron donating photosensitizer. To enhance the stacking interactions between an end-labeled pyrene moiety and the DNA base, *N*-methyl-*N*-pyrenylglycine was connected with a threoninol backbone[42] to afford the donor unit ^{A}Py (Figure 2 and Scheme S1, Supporting Information).

Charge Separation in Dyad Conjugates. To examine the effect of nucleobases flanking ^{A}Py on the fluorescence and the transient absorption spectra, dyad conjugates between ^{A}Py and deoxynucleotide were also synthesized (^{A}Py·N, N = A, C, G, or T, Figure 2). The fluorescence of ^{A}Py was strongly quenched by T and C in accord with the anticipated occurrence of exergonic intramolecular EET[43] from the ^{A}Py singlet state to pyrimidine bases, whereas virtually no fluorescent quenching was observed in the case of ^{A}Py·G (Supporting Information Figure S1 and Table 1).

Transient absorption spectra in the picosecond region were obtained during the laser flash photolysis using 360 nm laser. In the case of ^{A}Py·T, the rapid decay of the 560 nm band derived from ^{A}Py* was fraught with the rise of the 507 nm band attributed to ^{A}Py$^{\bullet+}$.The temporal variation of the subpicosecond transient absorption spectra from ^{A}Py·T can be also attributed to the charge separation between the ^{A}Py and T, followed by charge recombination (Figure 3). In the case of ^{A}Py·G, the growth of the 507 nm band was not observed, indicating the deactivation process does not include charge separation. Charge separation upon photoexcitation was observed with ^{A}Py·C but not with ^{A}Py·A. The observed rates were summarized in Table 1. Taken together, the photoexcitation of ^{A}Py results in an electron injection into DNA bases but not a hole injection.

Electron Injection to DNA. To monitor the initial electron injection process into DNA directly, ^{A}Py was covalently linked to 5′-end of hairpin conjugates possessing a GAA loop (hairpin **5**, for example), which makes extraordinary stable hairpin

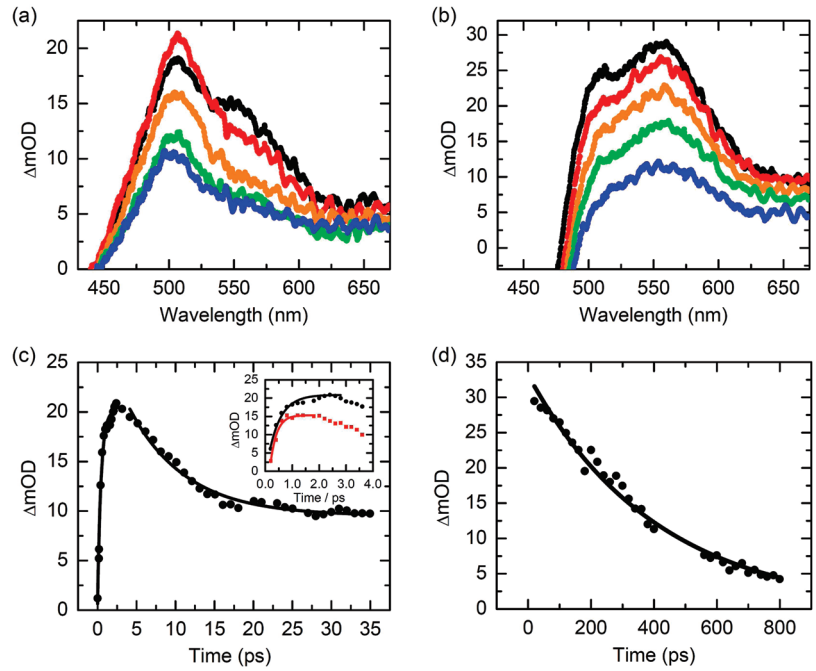

Figure 3. Temporal variation of the subpicosecond transient absorption spectra of (a) ^{A}**Py**·T dyad in the time range from 2 (black) to 20 ps (blue) and (b) ^{A}**Py**·G dyad in the time range from 10 (black) to 400 ps (blue) in 20 mM sodium phosphate and 100 mM sodium chloride (pH 7.0) (with 10% methanol in ^{A}**Py**·G solution) excited at 360 nm. Decay profiles of (c) ^{A}**Py**·T dyad monitored at 507 nm and (d) ^{A}**Py**·G dyad monitored at 560 nm after laser-pulse excitation. Inset indicates the decay profile of ^{A}**Py**·T dyad monitored at 507 (black) and 560 nm (red) in the early stage.

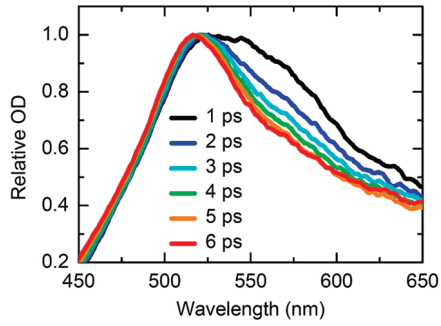

Figure 4. Temporal variation of the normalized transient absorption spectra of hairpin **5** in 20 mM sodium phosphate and 100 mM sodium chloride (pH = 7.0) in the time range from 1 (black) to 6 ps (red) excited at 360 nm with subpicosecond time resolution.

formation.[44] In the hairpin **5** (Figure 4), an excess electron injection could be also accomplished effectively by the photoexcitation of ^{A}**Py**, analogous to the ^{A}**Py**·T. The transient absorption spectra of hairpin **5** displayed a rapid decay of the 560 nm band originated from ^{A}**Py*** within a few picoseconds, and the following rise of the 510 nm band because of ^{A}**Py**$^{\bullet+}$ in the electron injection process. Nevertheless, the rapid charge recombination of the ^{A}**Py**$^{\bullet+}$·T$^{\bullet-}$ contact radical ion pair (τ_{CR} = 13 ps) suggests that the back electron transfer would be a predominant deactivation process of ^{A}**Py**$^{\bullet+}$.

Next, the effect of the insertion of ^{D}**T** between ^{A}**Py** and T is examined. In Figure 5a, fluorescence intensity of hairpins with or without ^{D}**T** was compared (hairpins **1**, **2**, and **4**). The quenching efficiency of ^{A}**Py** emission was decreased notably in the presence of ^{D}**T**·A base pair. Although pyrene-flurescence quenching by ^{D}**T** was reporeted,[45] the introduction of ^{D}**T** between ^{A}**Py** and T contributed to the enhancement of the fluorescence emission[39] and the efficient electron arrival in our hairpin system as seen in Figure 5b, which compares the kinetic trace of ΔO.D. attributable to both ^{A}**Py** radical cation and **DPA** radical anion. These results indicate that insertion of ^{D}**T** between ^{A}**Py** and T cause the delay of the initial charge recombination rate, and result in the enhancement of the yield for electron arrival to **DPA** as discussed in the later section using Figure 7.

Similar to hairpin **5**, the transient absorption spectra of hairpin **7** displayed a rapid decay of the 560 nm band originated from ^{A}**Py*** within a few picoseconds, and the following rise of the 510 nm band resulting from ^{A}**Py**$^{\bullet+}$ in the electron injection process (Figure 6). Meanwhile, the charge recombination rate of ^{A}**Py**$^{\bullet+}$ was considerably delayed by the insertion of a spacer base pair (τ_{CR} = 51 ps, Figure 6b). This result consistent with results observed in Figure 5. The amount of photoinduced degradation via iminium cation as an intermediate was examined in Figure 6c. The photodegradated product of hairpin **7** increased more than 4-fold compared with that of hairpin **5** (Figure 6c). Since the major photodegradated product was characterized as a hairpin conjugate tethering *N*-glyoxylyl threoninol moiety by MALDI-TOF MS (Supporting Information Figure S2), ^{A}**Py**$^{\bullet+}$ in hairpin **7** would be hydrolyzed via iminium cation according to the reaction mechanism indicated in Figure S2, Supporting Information. These results indicate that retardation of charge recombination by the insertion of ^{D}**T** enhanced possibility of charge injection by irreversible manner, although the actual rate and yield of photodegradation of ^{A}**Py** in DNA could not be determined from the estimated data.

Spectroscopic Observation of Excess Electron Arrival Process through DNA. To monitor the excess electron arrival process, **DPA** chromophore, which possesses lower reduction potential (E_{red} = −1.75 V vs NHE)[33] than those of the four nucleobases, in particular T (E_{red} = −1.8 V vs NHE), was designed as an electron acceptor and introduced into a hairpin bridge instead of GAA loop (Figure 1). The photoexcitation of hairpin conjugates containing **DPA** would be suspected of causing hole-injection into DNA.[33,34] The absorption band of ^{A}**Py** in the ground state extends to longer wavelength side than that of **DPA** (Supporting Information Figure S3). Furthermore, almost no transient signal was observed for the hairpin **10**

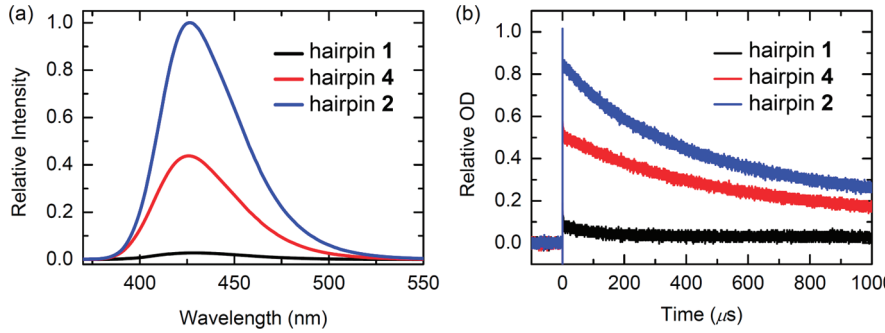

Figure 5. (a) Fluorescence spectra of hairpin **1** (without ^{D}**T**, black), **4** (with one ^{D}**T**, red), and **2** (with two ^{D}**T**, blue) in 20 mM sodium phosphate and 100 mM sodium chloride (pH = 7.0) excited at 360 nm and (b) the time profiles of hairpin **1** (black), **4** (red), and **2** (blue) in 20 mM sodium phosphate and 100 mM sodium chloride (pH = 7.0) monitored at 490 nm after irradiation of ^{A}**Py** with a 355-nm laserflash.

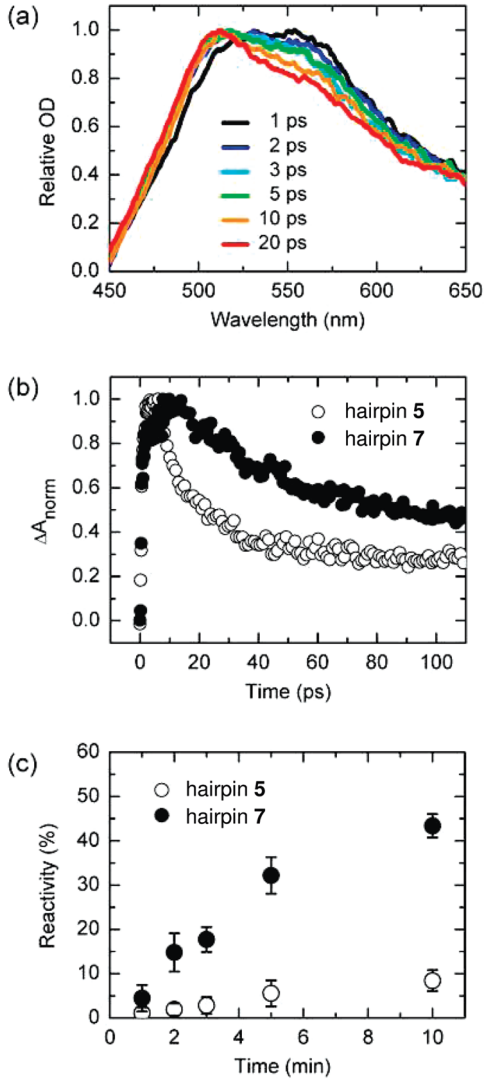

Figure 6. (a) Temporal variation of the normalized transient absorption spectra of hairpin **7** in the time range from 1 (black) to 20 ps (red) excited at 360 nm with subpicosecond time resolution. (b) Decay profiles of hairpin **5** (open circle) and hairpin **7** (filled circle) monitored at 505 nm after laser-pulse excitation. (c) Time profiles for the laser-induced decomposition of hairpin **5** (open circle) and hairpin **7** (filled circle) with the third-harmonic oscillation (355 nm, full width at half-maximum of 4 ns, 100 mJ per pulse) from a Q-switched Nd:YAG laser. After laser irradiation, the yields of photoinduced degradation of hairpins were analyzed by HPLC.

containing G·C base pair as a hole acceptor instead of ^{A}**Py** (Figure 7b). Thus, the hole injection was negligible upon excitation of our hairpins with a 355- or 360- nm laser pulse.

Unfortunately, the rising signal of **DPA**$^{\bullet-}$ was not observed in the sub-picosecond laser flash photolysis, even when the transient spectra was measured until 2 ns (our instrumental limitation). Figure 7a shows the nanosecond transient absorption spectra observed for hairpin **7** and hairpin **8** at 1 μs after a 355-nm laser flash. Substitution of **DPA**-bridge for GAA-loop in the hairpin enhanced transient absorption remarkably. The difference spectra between hairpin **7** and hairpin **8** displayed a characteristic transient signal with a peak at 500 nm and a shoulder at 450 nm assigned to **DPA**$^{\bullet-}$, which corresponded to the EET through DNA, suggesting that an excess electron migrates along the DNA to reach **DPA** site. Since the time resolution of ns instrument is a few tens nanosecond, generation time of DPA radical anion should be a few or a few tens nanoseconds, which is consistent with the previous assumption.[10,13,26] Thus, the lowest limit of hopping rate of excess electron between T·T will be 10^8 s^{-1}.

The decay profile of hairpin **8** monitored at 500 nm persisted over 100 μs (Figure 7a inset) indicating that charge recombination by an intermolecular collisional process should be participated.[31] Additionally, there are no significant signals in the 500−700 nm region (Figure 7a) and only a slight decrease of transient signals in hairpin **8** was observed even in the saturated N_2O, which is a well-known quencher for hydrated electrons (Supporting Information Figure S4). As indicated above, electron transfer from ^{A}**Py** to the solvent can be ignored also from the absence of radical cation formation of ^{A}**Py**·G. Thus, hydrate electrons via the two-photon ionization of pyrene moiety contribute little to the diffusive reduction of **DPA**$^{\bullet-}$ in our system.

Figure 7b indicates the signal intensity of other hairpins monitored at 500 nm and 1 μs after laser-pulse excitation. The relative ΔA of hairpins **5**−**9** indicates that separating the ^{A}**Py** and the adjacent T by a spacer definitively contributed to the signal enhancement of **DPA**$^{\bullet-}$. Siegmund et al. reported that a hairpin possessing a similar tethered 5′-pyrene group adopt an intercalated geometry rather than an end-capped one.[29] In the present hairpins, ^{A}**Py** seems not to be intercalated. If pyrene was intercalated between the first and second base pairs, relative ΔA of hairpins **6** and **7** would be the same. We have to point out that lower planarity of ^{D}**T** compared to T possibly weaken the π-stacking with ^{A}**Py** favorable to end-capping geometry.

The difference of the transient signals between **DPA**-bridged hairpin and GAA-looped hairpin represents the apparent quantum yield of electron arrival at **DPA** site (Φ_{EA}, Figure 7c). In addition to hairpin **8**, the decay profiles of all other hairpins are not accompanied by the rise of **DPA**$^{\bullet-}$ within the time resolution of our experimental setup. Alternatively, Φ_{EA} are moderately sequence-dependent, and especially mismatch-

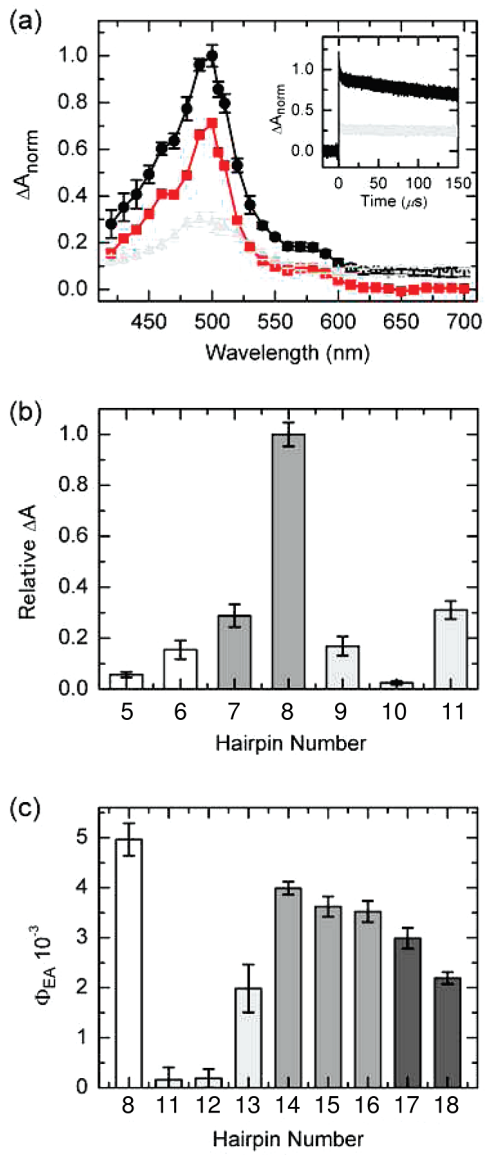

Figure 7. (a) Nanosecond time-resolved absorption spectra of hairpin **7** (gray) and hairpin **8** (black) monitored at 1 μs after the excitation of ^{A}**Py** with a 355 nm laser-pulse. The red is the difference spectrum. Inset: Time profiles observed at 490 nm in the hairpin **7** (gray) and hairpin **8** (black) after irradiation of ^{A}**Py** with a 355-nm laserflash. (b) The relative intensities of transient signals in a series of hairpins monitored at 1 μs and 490 nm after the excitation of ^{A}**Py** were analyzed to evaluate the effect of the spacer and the electron acceptor. In the presence of a spacer (gray), a significant enhancement of the transient absorption by the introduction of **DPA** compared with those in the absence of a spacer (white). Light gray group represents negative controls; the insertion position of the spacer (hairpin **9**), the contribution of photoinduced hole transfer (hairpin **10**), and the effect of a single base pair mismatch (hairpin **11**). (c) The difference of transient signals between each hairpin with **DPA** and hairpin **7** without **DPA** indicates the actual transient absorption of **DPA**$^{\bullet-}$. The apparent quantum yields (Φ_{EA}s) of electron arrival at **DPA** site were determined by comparing the obtained transient absorption of **DPA**$^{\bullet-}$ monitored at 1 μs and 490 nm with that of benzophenone, which was used as an actinometer, observed after the laser-pulse excitation. Φ_{EA} of hairpin **8** composed of only T·A base pairs (white) was compared with different categorized hairpin conjugates containing a single base pair mismatch (light gray), C·G base pairs (gray), and G·C base pairs (dark gray) in the bridge sequence.

sensitive. It is interesting to note that Φ_{EA}s of the hairpin **11** and **12** with a T·C and T·T mismatch were dramatically depressed and even comparable to that of GAA-looped hairpin,

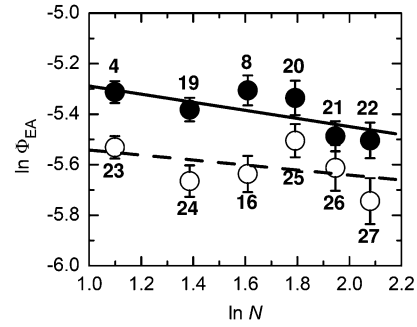

Figure 8. Distance dependences on the quantum yield of electron arrival (Φ_{EA}). The plots show ln(Φ_{EA}) for consecutive T (hairpin **4**, **8** and **19**−**22**, filled circle) and C (hairpin **16** and **23**−**27**, open circle) hairpins against the ln(N), where N is the number of hopping steps. The numbers close to the data points indicate the hairpin numbers.

whereas Φ_{EA} of hairpin **13** with a more stable T-G mismatch was somewhat higher than that of others. Besides the HT process, EET process also exhibited an extremely high sensitivity to the perturbation of π-stacking of the intervening DNA bases. In the case of HT, it was revealed that an orphan hole escaped from charge recombination successfully migrated to the hole acceptor through the mismatch site, but the hole-transfer rate was considerably decreased in the presence of the mismatch site.[31] In the case of EET, the introduction of the mismatch site decreased Φ_{EA} in EET, while retardant effect by mismatch was not detectable with the kinetic trace during the nanosecond laser flash photolysis, indicating that the substantially shorter duration of excess electrons in DNA ($<10^{-8}$ s), even when the excess electron migrates through the mismatch site.

Replacement of T·A base pair with C·G base pair has a much lesser, but still negative, effect on Φ_{EA}. The Φ_{EA} of hairpins with C·G base pairs decreased nonlinearly with increase of the number of C·G base pairs, and the Φ_{EA} of hairpin **15** with two C·G base pairs is approximately equal to that of consecutive C hairpin **16**, indicating that the efficiency as the electron trap is not significant like G as an hole trap. This result probably comes from small difference of the reduction potentials of T and C.[37] Moreover, the obtained Φ_{EA}s from consecutive T- and C-hairpins depended little on the distance and exhibited different linear correlations, respectively (Figure 8). This result indicates that EET migrates over 34 Å for both consecutive T and C sequences, which corresponds to the longest sequence investigated in this study.

As previously reported, a T base would act as a more effective electron carrier than a C base.[46] The rapid protonation of C radical anion might cause the slow down of the EET rate.[47] Hence, the nonlinear decrease of Φ_{EA} can be attributed to the involvement of the electron transfer process via C bases in the rate-determining step of EET in polypyrimidine hairpins. Actually, the Φ_{EA}s of hairpin **17** and **18** with T-G-T sequence, which is expected to show slower EET rate because of the lowest reduction potential of G, were slightly lower than those of polypyrimidine hairpins, and also affected more remarkably by the first substitution of T·A base pair with G·C base pair rather than by the second one. It is conceivable that the excess electron transfer for T-G-T sequence may be, in turn, the rate-determining step of EET.

Conclusion

In the present paper, we suggested that EET through DNA completed within a few or a few tens nanoseconds even for EET over 34 Å for both consecutive T and C sequences, which

corresponds to the longest sequence investigated in this study. The quantum yield of electron arrival displayed a relatively weak sequence dependence compared with the HT process. This trend is in accordance with previous results.[11−13,17−20,28] The fast and sequence-independent dynamics of EET lacking DNA damage is potentially promising for the development of electronic nanowires.

Acknowledgment. This work has been partly supported by a Grant-in-Aid for Scientific Research (Project 17105005, 21350075, 22245022, Priority Area (477), and others) from the Ministry of Education, Culture, Sports, Science and Technology (MEXT) of Japanese Government. T.M. thanks to WCU (World Class University) program through the National Research Foundation of Korea (MEST) (R31-10035) for the support.

Supporting Information Available: Synthetic scheme and method, fluorescence spectra of dyads, HPLC chart, absorption spectra of hairpins, and kinetic trace of Δo.d. during laser flash photolysis. These materials are available free of charge via the Internet at http://pubs.acs.org.

References and Notes

(1) Porath, D.; Bezryadin, A.; de Vries, S.; Dekker, C. *Nature* **2000**, *403*, 635–638.
(2) Lewis, F. D.; Liu, X.; Liu, J.; Miller, S. E.; Hayes, R.; Wasielewski, M. R. *Nature* **2000**, *406*, 51–53.
(3) Kelley, S. O.; Barton, J. K. *Science* **1999**, *283*, 375–381.
(4) Giese, B.; Amaudrut, J.; Kohler, A. K.; Spormann, M.; Wessely, S. *Nature* **2001**, *412*, 318–320.
(5) Henderson, P. T.; Jones, D.; Hampikian, G.; Kan, Y.; Schuster, G. B. *Proc. Natl. Acad. Sci. U.S.A.* **1999**, *96*, 8353–8358.
(6) Giese, B. *Annu. Rev. Biochem.* **2002**, *71*, 51–70.
(7) Wagenknecht, H. A. *Nat. Prod. Rep.* **2006**, *23*, 973–1006.
(8) Schwogler, A.; Burgdorf, L. T.; Carell, T. *Angew. Chem., Int. Ed.* **2000**, *39*, 3918–3920.
(9) Behrens, C.; Ober, M.; Carell, T. *Eur. J. Org. Chem.* **2002**, 3281–3289.
(10) Giese, B.; Carl, B.; Carl, T.; Carell, T.; Behrens, C.; Hennecke, U.; Schiewmann, O.; Feresin, E. *Angew. Chem., Int. Ed.* **2004**, *43*, 1848–1851.
(11) Behrens, C; Burgdorf, L. T.; Schwogler, A.; Carell, T. *Angew. Chem., Int. Ed.* **2002**, *41*, 1763–1766.
(12) Behrens, C.; Cichon, M. K.; Grolle, F.; Hennecke, U.; Carell, T. *Top. Curr. Chem.* **2004**, *236*, 187–204.
(13) Breeger, S.; Hennecke, U.; Carell, T. *J. Am. Chem. Soc.* **2004**, *126*, 1302–1303.
(14) Carell, T.; Behrens, C.; Gierlich, J. *Org. Biomol. Chem.* **2003**, *1*, 2221–2228.
(15) Ito, T.; Rokita, S. E. *J. Am. Chem. Soc.* **2003**, *125*, 11480–11481.
(16) Ito, T.; Rokita, S. E. *J. Am. Chem. Soc.* **2004**, *126*, 15552–15529.
(17) Stafforst, T.; Diederichsen, U. *Angew. Chem., Int. Ed.* **2006**, *45*, 5376–5380.
(18) Shao, F.; Elias, B.; Lu, W.; Barton, J. K. *Inorg. Chem.* **2007**, *46*, 10187–10199.
(19) Shao, F.; Barton, J. K. *J. Am. Chem. Soc.* **2007**, *129*, 14733–14738.
(20) Elias, B.; Shao, F.; Barton, J. K. *J. Am. Chem. Soc.* **2008**, *130*, 1152–1153.
(21) Yamagami, R.; Kobayashi, K.; Tagawa, S. *Chem.—Eur. J.* **2009**, *15*, 12201–12203.
(22) Lewis, F. D.; Liu, X.; Miller, S. E.; Hayes, R. T.; Wasielewski, M. R. *J. Am. Chem. Soc.* **2002**, *124*, 11280–11281.
(23) Gaballah, S. T.; Hussein, Y. H.; Anderson, N.; Lian, T. T.; Netzel, T. L. *J. Phys. Chem. A* **2005**, *109*, 10832–10845.
(24) Gaballah, S. T.; Vaught, J. D.; Eaton, B. E.; Netzel, T. L. *J. Phys. Chem. B* **2005**, *109*, 5927–5934.
(25) Amann, N.; Pandurski, E.; Fiebig, T.; Wagenknecht, H. A. *Angew. Chem., Int. Ed.* **2002**, *41*, 2978–2980.
(26) Kaden, P.; Mayer-Enthart, E.; Trifonov, A.; Fiebig, T.; Wagenknecht, H. A. *Angew. Chem., Int. Ed.* **2005**, *44*, 1636–1639.
(27) Valis, L.; Wang, Q.; Raytchev, M.; Buchvarov, I.; Wagenknecht, H. A.; Fiebig, T. *Proc. Natl. Acad. Sci. U.S.A.* **2006**, *103*, 10192–10195.
(28) Daublain, P.; Thazhathveeti, A. K.; Wang, Q.; Trifonov, A.; Fiebig, T.; Lewis, F. D. *J. Am. Chem. Soc.* **2009**, *131*, 16790–16797.
(29) Siegmund, K.; Daublain, P.; Wang, Q.; Trifonov, A.; Fiebig, T.; Lewis, F. D. *J. Phys. Chem. B* **2009**, *113*, 16276–16284.
(30) Kawai, K.; Kimura, T.; Kawabata, K.; Tojo, S.; Majima, T. *J. Phys. Chem. B* **2003**, *107*, 12838–12841.
(31) Takada, T.; Kawai, K.; Fujitsuka, M.; Majima, T. *Proc. Natl. Acad. Sci. U.S.A.* **2004**, *101*, 14002–14006.
(32) Schulhof, J. C.; Molko, D.; Teoule, R. *Nucleic Acids Res.* **1988**, *16*, 319–326.
(33) Lewis, F. D.; Liu, X.; Miller, S. E.; Hayes, R. T.; Wasielewski, M. R. *J. Am. Chem. Soc.* **2002**, *124*, 14020–14026.
(34) Takada, T.; Kawai, K.; Fujitsuka, M.; Majima, T. *Angew. Chem., Int. Ed.* **2006**, *45*, 120–122.
(35) Takada, T.; Kawai, K.; Cai, X.; Sugimoto, A.; Fujitsuka, M.; Majima, T. *J. Am. Chem. Soc.* **2004**, *126*, 1125–1129.
(36) Kawai, K.; Osakada, Y.; Fujitsuka, M.; Majima, T. *J. Phys. Chem. B* **2008**, *112*, 2144–2149.
(37) Seidel, C. A. M.; Schulz, A.; Sauer, M. H. M. *J. Phys. Chem.* **1996**, *100*, 5541–5553.
(38) Ide, H.; Wallace, S. S. *Nucleic Acids Res.* **1988**, *16*, 11339–11354.
(39) Wilson, J. N.; Cho, Y.; Tan, S.; Cuppoletti, A.; Kool, E. T. *ChemBioChem* **2008**, *9*, 279–285.
(40) Leon, J. W.; Whitten, D. G. *J. Am. Chem. Soc.* **1993**, *115*, 8038–8043.
(41) Yoon, U. C.; Su, Z.; Mariano, P. S. In *CRC Handbook of Organic Photochemistry and Photobiology*, 2nd ed.; Horspool, W., Lenci, F., Eds.; CRC Press: Boca Raton, 2004; pp 101/1−101/20.
(42) Takarada, T.; Tamaru, D.; Liang, X.; Asanuma, H.; Komiyama, M. *Chem. Lett.* **2001**, *30*, 732–733.
(43) From the oxidation potential of 1.3 V (vs. NHE in CH_3CN) for ^{A}**Py** and the excitation energy of 3.2 eV for ^{A}**Py** in the singlet excited state (^{1A}**Py***), oxidation potential of ^{1A}**Py*** is calculated to be −1.9 eV. Because a high oxidation potential of ^{1A}**Py*** is enough to reduce pyrimidine bases (redox potentials of C and T are −1.9 and −1.8 V, respectively),[37] the charge separation between ^{1A}**Py*** and pyrimidine bases is expected to occur after the excitation of the ^{A}**Py** site when ^{A}**Py** was stacked with DNA bases.
(44) Yoshizawa, S.; Kawai, G.; Watanabe, K.; Miura, K.; Hirao, I. *Biochemistry* **1997**, *36*, 4761–4767.
(45) Scannell, M. P.; Prakash, G.; Falvey, D. E. *J. Phys. Chem. A* **1997**, *101*, 4332–4337.
(46) Wagner, C.; Wagenknecht, H. A. *Chem.—Eur. J.* **2005**, *11*, 1871–1876.
(47) Cai, Z.; Li, X.; Sevilla, M. D. *J. Phys. Chem. B* **2002**, *106*, 2755–2762.

JP1024685